



THE UNIVERSITY *of* EDINBURGH

Edinburgh Research Explorer

Emergence of Molecular Recognition Phenomena in a Simple Model of Imprinted porous Materials

Citation for published version:

Dourado, EMA & Sarkisov, L 2009, 'Emergence of Molecular Recognition Phenomena in a Simple Model of Imprinted porous Materials', *Journal of Chemical Physics*, vol. 130, no. 21, pp. 214701.

Link:

[Link to publication record in Edinburgh Research Explorer](#)

Document Version:

Peer reviewed version

Published In:

Journal of Chemical Physics

General rights

Copyright for the publications made accessible via the Edinburgh Research Explorer is retained by the author(s) and / or other copyright owners and it is a condition of accessing these publications that users recognise and abide by the legal requirements associated with these rights.

Take down policy

The University of Edinburgh has made every reasonable effort to ensure that Edinburgh Research Explorer content complies with UK legislation. If you believe that the public display of this file breaches copyright please contact openaccess@ed.ac.uk providing details, and we will remove access to the work immediately and investigate your claim.



Emergence of molecular recognition phenomena in a simple model of imprinted porous materials

Eduardo M. A. Dourado and Lev Sarkisov^{a)}

*Institute for Materials of Processes, The University of Edinburgh, King's Buildings,
Mayfield Road, EH9 3JL Edinburgh, United Kingdom*

(Received 25 February 2009; accepted 24 April 2009; published online xx xx xxxx)

Polymerization in the presence of templates, followed by their consequent removal, leads to structures with cavities capable of molecular recognition. This molecular imprinting technology has been employed to create porous polymers with tailored selectivity for adsorption, chromatographic separations, sensing, and other applications. Performance of these materials crucially depends on the availability of highly selective binding sites. This parameter is a function of a large number of processing conditions and is difficult to control. Furthermore, the nature of molecular recognition processes in these materials is poorly understood to allow a more systematic design. In this work we propose a simple model of molecularly imprinted polymers mimicking the actual process of their formation. We demonstrate that a range of molecular recognition effects emerge in this model and that they are consistent with the experimental observations. The model also provides a wealth of information on how binding sites form and function in the imprinted structures. It demonstrates the capability to assess the role of various processing conditions in the final properties of imprinted materials, and therefore it can be used to provide some qualitative insights on the optimal values of processing parameters. © 2009 American Institute of Physics. [DOI: 10.1063/1.3140204]

I. INTRODUCTION

Molecular recognition is a process of strong and specific noncovalent binding between a molecule and a substrate. This mechanism is vital for a number of biological processes including enzymatic reactions, defensive mechanisms, and genetic information replication. Recently, however, a technology has been developed to synthesize abiogenic porous structures capable of biomimetic molecular recognition. At the heart of this technology is the molecular imprinting protocol, where self-assembly of the precursors and polymerization of the material take place in the presence of additional template molecules. The templates are subsequently removed leaving in the final structure cavities, or imprints, which are structurally complementary to the template species. These cavities function as selective binding sites, capable of recognition and rebinding of the original template species. The first observation of molecular recognition in abiogenic structures dates back to 1931, when Polyakov¹ prepared sol-gel materials in the presence of benzene, toluene, and xylene and observed a particular affinity of the resulted structures toward the original additives or related ligands. It was hypothesized that the produced silica materials acquired some kind of *steric memory* toward the guest species. However, the true potential of this approach was realized with the first molecularly imprinted polymers (MIPs) prepared in 1970s.² In MIP synthesis, the polymerizing mixture consists of cross-linker component, responsible for the structural integrity of the polymer, and functional monomers, which form associations with the functional groups of the template molecule. Thus, in addition to steric effects, the resulting binding site also fea-

tures very specific complementary interaction patterns. The basic steps of this technique are shown in Fig. 1. For example, one of the earliest MIPs was prepared using methacrylic acid as the functional monomer and ethylene glycol dimethacrylate as the cross-linking monomer, with two small drug molecules, theophylline and diazepam, as the template species.³ These structures were able to differentiate between close analogs of the template, exhibiting properties similar to the natural antibodies. This demonstrated the remarkable potential of molecular imprinting. Rich polymeric chemistry and a large number of possible building components opened an opportunity to design highly functionalized materials for chromatographic separations, sensing, artificial immunoassays, catalysis, and other applications implemented over the last 20 years.²

Despite these successes, synthesis of MIPs remains an intricate and vastly empirical process.⁴ It has been well established in a number of studies that MIPs have few selective binding sites and a large number of relatively nonselective sites.⁵ This heterogeneity of binding sites is an intrinsic feature of the imprinting technique. The performance of a MIP crucially depends on this characteristic, and it is important to be able to control it. For this we need a detailed understanding of how specific binding sites form and function.

Recent experimental and theoretical studies suggest that very selective, high quality binding sites result from strong associations between the functional monomers and template species.^{6–10} For example, in the aforementioned study by Vlatakis *et al.*,³ methacrylic acid forms ionic interactions and hydrogen bonds with amino and polar functional groups of the template. Naturally, most of the recent design efforts have been focused on screening for appropriate functional

^{a)}Electronic mail: lev.sarkisov@ed.ac.uk.

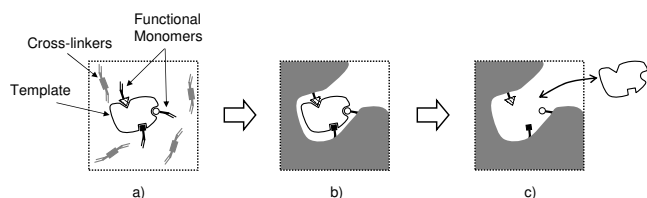


FIG. 1. A schematic depiction of the polymer imprinting principles. (a) A mixture of components is equilibrated and functional monomer-template complexes are formed; (b) polymerization stage; (c) after template extraction, a cavity is left capable of rebinding the template.

monomers associated with it. This leads to binding sites of different types and quality, depending on the number of monomers associated with the site. This model is clearly well suited to explore binding site distributions in MIPs and how this characteristic depends on the relative concentrations of the template and monomer species and on the strength of the template-functional monomer association. It was also applied to a specific case of enantioselective recognition of racemic components. It is also important to note that a number of atomistic models of MIPs have started to emerge recently.

In this work, we aim to develop a more general, computationally efficient model, which would satisfy the following criteria. The model should reflect the process of MIP formation and feature complex interconnected three dimensional porous space characteristic for MIPs. The model should exhibit molecular recognition and provide a tool to investigate the relation between various processing conditions (such as relative concentration of species), porous morphology, and the binding site distribution. Several elements of this strategy have been already developed. Van Tassel *et al.* proposed a series of models, where all species were represented as hard spheres or Lennard-Jones particles. The first step of the model involves an equilibrated mixture of template and matrix components (matrix here and throughout the article is a generic term for the polymer components). The mixture is then quenched and the template particles are removed. The resulting structure of the quenched matrix component serves as the model porous material. The advantage of the model is that it also allows for a theoretical treatment within the replica Ornstein-Zernike formalism. It has been shown that the presence of a template enhances adsorption and that the magnitude of the effect strongly depends on the template/matrix composition ratio and on the size of the template. However, as expected, no molecular recognition effect could be captured in a system of simple particles. Recently, the model of Van Tassel *et al.* was extended to molecular species. Using both computer simulations and integral equation approaches, a range of systems with either purely repulsive or more complex patterns of interaction was considered. The adsorption of rigid linear chains, clusters, and molecules of other shapes in matrices templated with these species was investigated and a number of nontrivial effects were observed. Molecular recognition was also observed for systems interacting with Lennard-Jones-like potentials; however, this observation was limited to one specific system in a narrow range of conditions and therefore it lacks generality.

II. METHODOLOGY

A. Computational strategy

In the first step a mixture of the MIP components (template, cross-linker, and functional monomer) is equilibrated under specified conditions. When equilibrium is reached, the system is quenched (i.e., molecules are frozen in their positions and orientations), this stage imitates polymerization in the actual MIP synthesis. The porous structure formed by the quenched configurations of the matrix species (cross-linkers

monomers, which would form stable complexes with the template molecule of interest. This, however, is only one of many factors that play a role in the final characteristics of a MIP. First of all, not all of the formed complexes become selective binding sites. Some of the complexes may be destroyed during the polymerization process, and others may evolve into inaccessible binding sites either because of a trapped template molecule inside or because they become spatially isolated from the remaining porous space during the polymerization. Furthermore, several scenarios are possible where specific and accessible binding sites are not able to perform their rebinding function. For example, during the adsorption or rebinding process, one or more molecules can form associations with the interaction groups of the binding sites in an arrangement different from the original predecessor complex. In general, recognition events in a binding site are strongly affected by the state of the neighboring binding sites and pores. All of these factors may contribute to the diminished performance of a MIP and are intimately linked to the various properties of the imprinted material such as density, concentration of the interaction groups on the surface, and so on. As a result MIP performance depends not only on the stability of the complexes between functional monomers and templates in the prepolymerization mixture but also on a number of other processing conditions such as relative concentration of the components, choice of solvent, and polymerization temperature. The number of optimization parameters is large, they are not independent of each other and their mutual effects are quite intricate. Clearly, design of MIPs with tailored functionalities requires some rational strategies.

Computational methods and theoretical approaches have been playing an increasingly important role in the development of these strategies with a number of fundamental models of MIPs recently proposed. For example, Yungerman and Srebnik considered a model of a polymerizing Lennard-Jones fluid templated with rigid dimers, also made of two Lennard-Jones sites. Polymerization was modeled as the formation of harmonic bonds between the particles representing monomers. This model allowed the authors to investigate porosity and pore size distribution in the final structure as function of the template concentration and degree of polymerization. Wu *et al.* recently proposed a simple two dimensional square lattice model of MIPs. In the model each lattice site can be either empty or occupied by a cross-linker, functional monomer, or template species. Each functional monomer can form an association with only one out of four adjacent lattice sites. Template sites can have up to four

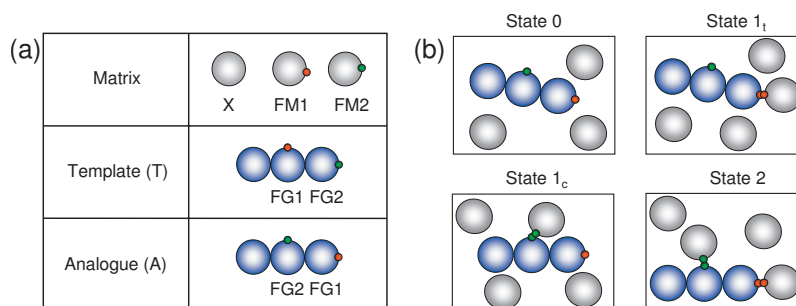


FIG. 2. (Color) (a) Summary of the species considered in this work. Matrix species include cross-linker X and functional monomers $FM1$ and $FM2$, which feature surface interaction sites shown in red ($FM1$) and green ($FM2$); template (T) is a rigid chain of three tangent hard spheres with surface interaction sites in the arrangement as shown. Functional group $FG1$ (red interaction site) can associate with functional monomer $FM1$, functional group $FG2$ (green interaction site) can associate with functional monomer $FM2$. Analog A has the location of the functional groups exchanged. (b) Schematic depiction of the possible complexes between the template and functional monomers in the prepolymerization mixture. Each complex is described by the number of associations formed between the template and functional monomers (states 0, 1, 1_c, 2), with subscripts t and c signifying the terminal and central location of the engaged functional group, respectively.

and functional monomers) models the MIP after template extraction. This simulated MIP is then used in the adsorption simulations.

B. Molecular model

In a series of earlier studies, Sarkisov and Van Tassel^{32,33} applied the strategy described above to a range of systems where rigid molecules were constructed from a basic building block, such as a hard sphere or a Lennard-Jones-like particle. For example, the template could be represented as a rigid chain of several hard spheres, whereas the polymer was represented simply as a fluid of hard spheres.

In order to capture the molecular recognition phenomena, we need to go beyond these types of interactions. In experiments, formation of the very specific binding sites results from strong associations between the template molecule and functional monomers. The nature of these associations is complex and includes both hydrogen bonds and electrostatic contributions. To a significant extent, molecular recognition is a process of reforming of these associations in the binding site. Thus, the idea of this work is to extend the model of Sarkisov and Van Tassel to incorporate a simple description of associations forming between functional monomers and a template molecule. The inspiration for our approach comes from an earlier model of water proposed by Kolafa *et al.*^{35,36} In their model, water is represented as a hard sphere decorated with four additional interaction sites in a tetrahedral arrangement. These interaction sites, located close to or at the surface of the hard sphere, are small compared to the central hard sphere particle and are able to associate with each other via a short range square-well potential. Associations between water particles in this description feature directionality, short range, and strength of hydrogen bonds. Using this approach we construct the species involved in our model as shown in Fig. 2(a). In this study, a cross-linker molecule is a hard sphere of size σ (species X). A functional monomer in this model is represented as a hard sphere of size σ with an interaction site on the surface as shown in Fig. 2(a). We consider functional monomers of two types, $FM1$ and $FM2$, but the model is not limited to this specific case. A template molecule (species T) is a rigid linear chain of three

tangent hard spheres of the same size σ . Two of these spheres also feature surface interaction sites in the arrangement as shown in Fig. 2(a) and can be viewed as functional groups ($FG1$ and $FG2$). Functional monomer $FM1$ can associate with functional group $FG1$, whereas functional monomer $FM2$ can associate with functional group $FG2$. The association between interaction sites is modeled via a square-well potential of the following form:

$$u(r)/k_B T = \begin{cases} -\varepsilon/k_B T, & r \leq \sigma_{SW} \\ 0, & r > \sigma_{SW}, \end{cases} \quad (1)$$

where $u(r)$ is the interaction energy between two interaction sites, r is the distance between the two sites, ε determines the well depth of the potential and is equal to $10k_B T$ (typical magnitude for hydrogen bonds), σ_{SW} is the size of the interaction site and is equal to 0.15σ , and k_B and T are the Boltzmann constant and temperature as usual. No functional monomers can associate with each other, and the same is true for the functional groups.

One of the key objectives of this study is to test whether the proposed model is capable of molecular recognition. This function would manifest itself in the ability of the model imprinted matrix to preferentially adsorb the original template species and distinguish them from analogous species that have similar structure and composition but different arrangements of the functional groups. An example of such an analog, where the location of the functional groups is exchanged, is also shown in Fig. 2(a).

C. Characterization of prepolymerization complexes and binding sites

In the model presented here, associations form between the functional monomers and the functional groups of the template. In the prepolymerization mixture composed from the species presented in Fig. 2(a), a template molecule can be observed in one of four possible states. These states are shown in Fig. 2(b). In the first state, labeled 0, the template molecule does not form any associations. States (or complexes) 1, and 1_c are characterized by a single association with either the terminal or the central functional group of the template engaged in the association, respectively. (We

choose this notation, instead of using FG1 and FG2, since the location of these groups in the template and analog molecules is swapped.) Finally, the template can have associations established with both functional groups and this corresponds to state (or complex of type) 2. Computer simulations allow us to monitor the population of these complexes during the equilibration of the matrix and relate these characteristics to various parameters of the system, such as composition and density. Once the system is quenched (imitating polymerization), the complexes are frozen in their instant configurations. Template removal transforms these complexes into binding sites.

Let us consider behavior of these binding sites during an adsorption process, where we use template as the adsorbate. Again, adsorbed molecules can be observed in different states, similar to those depicted in Fig. 2(b), depending on the number of associations they form with the matrix. It is important to recognize that not all of these states correspond to molecules located in the binding sites formed during the imprinting. For example, a situation is possible where an adsorbing molecule is able to form two associations with the matrix in an arrangement that does not correspond to any particular complex in the prepolymerization mixture. Thus, to distinguish the states of the adsorbed molecules from those in the prepolymerization mixture, we introduce a classification of adsorbed states similar to that in Fig. 2(b) and based simply on the number of associations the adsorbed molecule forms with the matrix. Specifically, molecules that form two associations with the matrix are denoted as state 2^a (“a” stands here for an adsorbed molecule here); a molecule with only one association made by the terminal functional group is in state 1_t^a ; a molecule with only one association made by the central functional group is in state 1_c^a ; finally a molecule with no associations is classified as state 0^a . It is instructive to know how many of the molecules in state 2^a are actually located in the binding sites resulted from the complexes of type 2 in the prepolymerization mixture. Computer simulations allow us, given a particular state on the adsorption isotherm, to examine the binding state of each molecule.

D. Simulation details

The first stage of the proposed computational strategy considers an equilibrium mixture of the template, functional monomer, and cross-linker components. Equilibration of the system is performed in the canonical NVT ensemble using the classical Metropolis sampling protocol. The number of canonical Monte Carlo steps (translations and rotations) required for the equilibration is between 3×10^8 and 6×10^8 (depending on the system), of these approximately 5×10^7 are used to generate average properties of the system. For each system, a total of three different matrix realizations are generated.

Simulations of adsorption are performed using the grand canonical Monte Carlo. In this ensemble, temperature T , volume of the system V , and the chemical potential $\mu/k_B T$ of the adsorbing species are specified. A point on the adsorption isotherm corresponds to a simulation with approximately 10^8

steps performed, with each step being either an insertion, deletion, translation, or rotation attempt. Translations and rotations are accepted with the acceptance probability,

$$P_{\text{trans,rot}} = \min(1, e^{-\beta[U_{\text{new}} - U_{\text{old}}]}), \quad (2)$$

where $\beta = 1/k_B T$, U_{old} , and U_{new} are the configurational energies of the system before and after the attempted move, respectively. To increase the efficiency of insertion and deletion moves, we implement a volume biased sampling method as described by Snurr *et al.*³⁷ in the context of adsorption in zeolites. In this method the system is divided into small cubelets. A probe hard sphere particle is placed in the center of each cubelet and tested for overlaps with the particles of the structure. If no overlaps are registered, this cubelet is saved in a list of accessible cubelets. Insertions are then performed by random selection of a cubelet from the list. A molecule of adsorbate is randomly placed within the selected cubelet, with this move accepted or rejected based on the following biased probability criterion:

$$P_{\text{ins}} = \min\left(1, \frac{q^{\text{rot}} e^{\beta \mu V_C}}{(N+1)\Lambda^3}\right), \quad (3)$$

where N is the number of adsorbate molecules in the system and V_C is the total volume of all accessible cubelets. Note that the de Broglie wavelength Λ and the ideal gas rotational partition function q^{rot} are implicitly set to σ and 1, respectively. In order to preserve the microscopic reversibility, the acceptance criterion for particle deletions also has to be biased,

$$P_{\text{del}} = \min\left(1, \frac{N\Lambda^3}{q^{\text{rot}} e^{\beta \mu V_C}}\right). \quad (4)$$

These simulations are carried out for a range of increasing values of chemical potential. The adsorbed density of the species as a function of the chemical potential constitutes an adsorption isotherm.

III. RESULTS

In this study, we explore six different MIP systems and their parameters are given in Table I. MIP1 has characteristics, such as the overall density, similar to those in the earlier studies of Sarkisov and Van Tassel.³³ This system features 2400 cross-linker particles and 400 functional monomer particles of each type. The system is imprinted with 400 template molecules. Therefore, the ratio of functional monomers ($N_{\text{FM1}} + N_{\text{FM2}}$) and functional groups ($N_{\text{FG1}} + N_{\text{FG2}}$) is stoichiometric in the system. The prepolymerization mixture is placed in a cubic box of 20σ in size. The overall reduced density of the system, $\rho^* = (N_{\text{total}}/V)\sigma^3$, is 0.55 (here $N_{\text{total}} = N_X + N_{\text{FM1}} + N_{\text{FM2}} + 3N_T$ is the total number of hard sphere particles present in the system, N_X and N_T is the number of cross-linker and template particles, V is the volume of the system).

The first step of the proposed protocol involves simulation of an equilibrium mixture of the cross-linker, functional monomers, and template components. Figure 3 summarizes the distribution of complexes observed in this prepolymerization mixture. About 25% of templates are able to form

TABLE I. Summary of the compositions and densities $\rho^* = (N_{\text{total}}/V)\sigma^3$ for the systems studied in this work. Here, N_{total} is the total number of hard sphere sites in the system, whereas N_X , N_{FM1} , N_{FM2} , and N_T are the number of cross-linker X, functional monomer FM1, functional monomer FM2, and template T particles, respectively.

MIP	N_X	N_{FM1}	N_{FM2}	N_T	ρ^*
1	2400	400	400	400	0.5500
2	1800	300	300	300	0.4125
3	3000	500	500	500	0.6875
4	2800	200	200	400	0.5500
5	1600	800	800	400	0.5500
6	0	1600	1600	400	0.5500

associations with two functional monomers. Other states of the template molecules (bound to just one monomer, either FM1 or FM2, or not bound to any functional monomers) are also observed with roughly the same probability of 25% for each state. The final configuration of this mixture is saved, the template species are removed, and the resulting structure represents a model MIP. The most intriguing aspect of this study is to establish whether this model material is capable of molecular recognition. For this we perform single component adsorption simulations of the template and analog. The analog, as depicted in Fig. 2(a), features exactly the same building blocks and the overall geometry as the template, however, the location of the interaction sites is reversed, compared to the template. Thus, higher adsorbed density of the template compared to the analog at the same corresponding chemical potential would signify molecular recognition in the model MIP. Figure 4(a) shows adsorption isotherms for the template and analog. Indeed, adsorption densities for the template are higher throughout the whole range of chemical potentials. A more intuitive way to characterize selectivity of a MIP is the separation factor S , which is the ratio of the adsorbed template and analog densities at the same chemical potential. This factor is plotted in Fig. 4(b). For the whole range of chemical potential, this factor is greater than 1, signifying the preferential adsorption of the template compared to the analog. As expected, this factor is decreasing at higher loadings, as the highly specific binding sites become occupied at lower chemical potentials and the remaining porous space does not exhibit any preferential adsorption. This trend is very similar to what is typically observed in experi-

ments, and even the values of the separation factor are comparable to the typical experimental values in MIP studies.⁵ Hence, we establish that the presented model is able to capture molecular recognition effect. Computer simulations allow us to generate a detailed look at the state of each adsorbed molecule and its environment throughout the whole adsorption process. Specifically, for each state on the adsorption isotherm, we have complete information about how many molecules form two associations with the matrix, just one association with the matrix, or have no associations formed at all. Figure 5(a) summarizes the distribution of adsorbed molecules among different states of association along the adsorption isotherm for MIP1. For example, at the

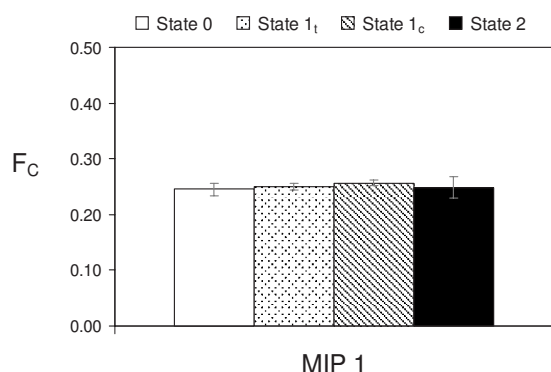


FIG. 3. Equilibrium distribution of the template-functional monomer complexes in MIP1 system prior to polymerization. F_C is the fraction of complexes of each type.

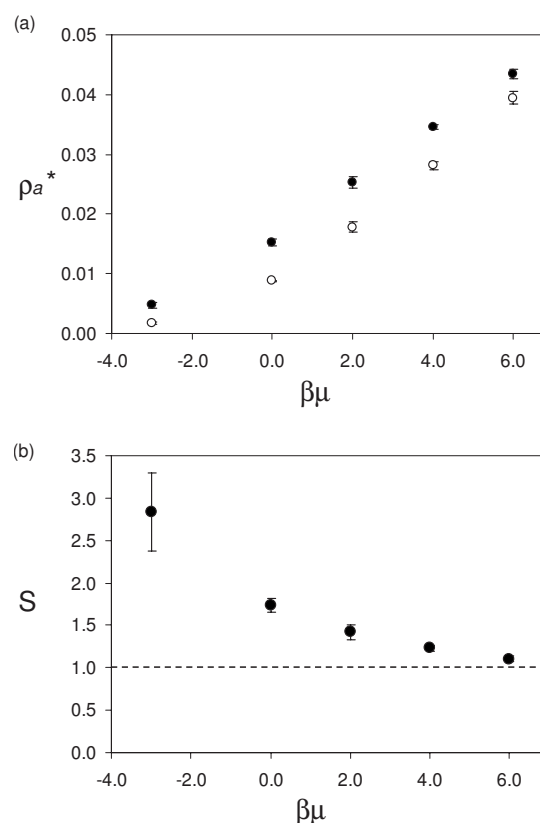


FIG. 4. (a) The adsorption isotherms for MIP1, adsorbate density $\rho_a^* = (N_a/V)\sigma^3$ as a function of the adsorbate chemical potential $\beta\mu$. N_a is the number of adsorbed molecules. Closed symbols correspond to the adsorbed template density $\rho_{a,T}^*$ and open symbols correspond to the adsorbed analog density $\rho_{a,A}^*$. (b) Separation factor $S = \rho_{a,T}^*/\rho_{a,A}^*$ as a function of the chemical potential $\beta\mu$ for MIP1.

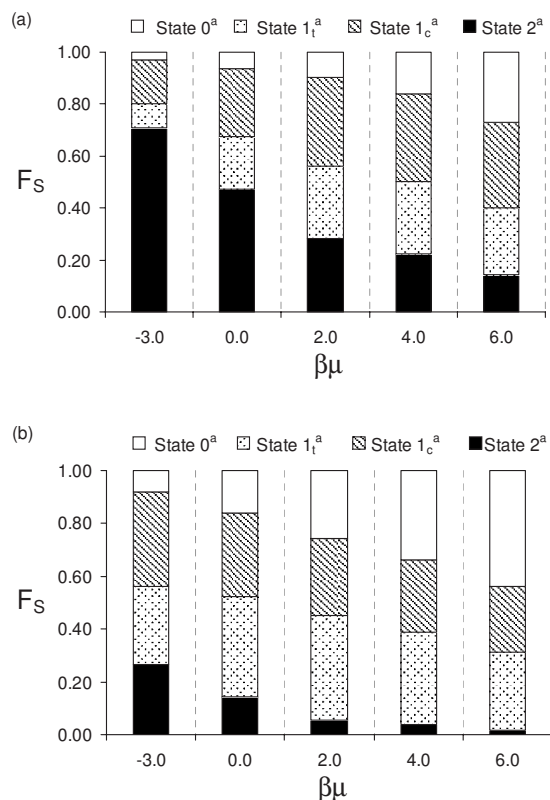


FIG. 5. Fraction F_S of adsorbed molecules in each binding state as a function of the chemical potential $\beta\mu$ in MIP1 for the template (a) and analog (b).

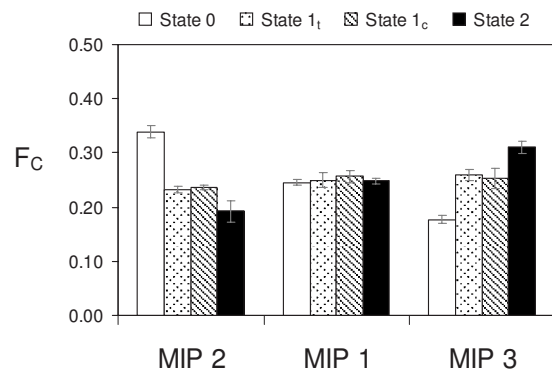


FIG. 6. Equilibrium distribution of the template-functional monomer complexes in MIP2 and MIP3 systems prior to polymerization, compared to this distribution in MIP1. F_C is the fraction of complexes of each type.

type 2 complexes observed in the mixture. High density of the mixture also induces stronger complementarity between the template and the resulting binding site. All these factors lead to higher selectivity in MIP3 compared to the materials of lower density. Figure 7 summarizes adsorption isotherms and separation factors for all three materials. Although, capacity of MIP3 is lower compared to other materials due to the reduced porosity, this system exhibits significantly higher separation factors reaching more than 7 at the lowest value of the chemical potential shown in the figure.

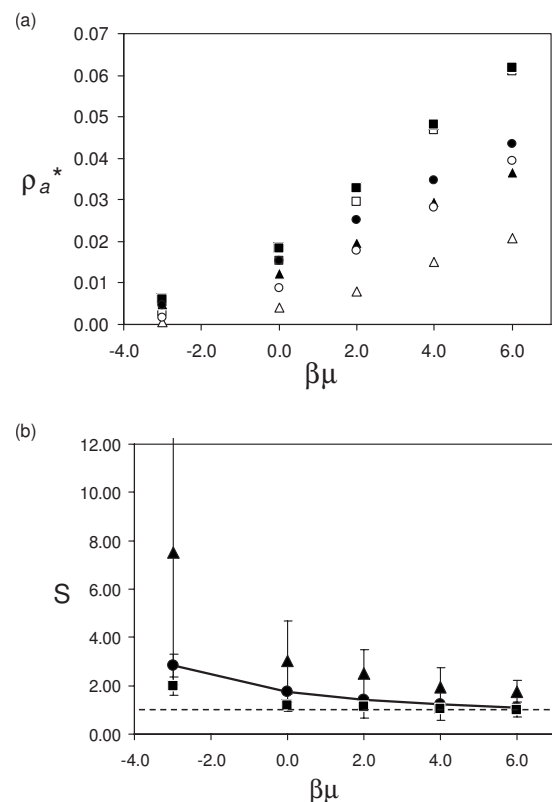


FIG. 7. (a) The adsorption isotherms for MIP1 (circles), MIP2 (squares), and MIP3 (triangles), adsorbate density $\rho_a^* = (N_a/V)\sigma^3$ as a function of the adsorbate chemical potential $\beta\mu$. N_a is the number of adsorbed molecules. Closed symbols correspond to the adsorbed template density $\rho_{a,T}^*$ and open symbols correspond to the adsorbed analog density $\rho_{a,A}^*$. Error bars are not shown for clarity. (b) Separation factor $S = \rho_{a,T}^*/\rho_{a,A}^*$ as a function of chemical potential $\beta\mu$ for MIP1 (circles and solid line), MIP2 (squares), and MIP3 (triangles).

chemical potential $\beta\mu = -3.0$, there are about 70% of adsorbed molecules in 2^a state, 9% in 1_i^a state, 18% in 1_c^a state, and 3% not forming any associations (state 0). Overall, at lower values of the chemical potential, the majority of the adsorbed molecules form two associations with the matrix. As the loading of the material increases, progressively more and more molecules are able to form only one association with the matrix or no associations at all. Interestingly, at the highest loading the distribution of binding sites among different association states resembles the distribution of complexes in the prepolymerization mixture. It is also instructive to apply similar analysis to the analog adsorption in the same material. Figure 5(b) shows distribution of adsorbed molecules among different binding states for the analog in MIP1. The most important feature of this result is a significant fraction of analog molecules that are able to form two associations with the matrix despite the porous space being specifically tailored to recognize the interaction pattern of the template.

In order to investigate the effect of density on molecular recognition in MIPs, we consider two variations of MIP1. Both of the systems feature the same mole fractions of the components as MIP1; however, MIP2 has lower overall density than MIP1 (75% of MIP1) and MIP3 has higher overall density than MIP1 (125% of MIP1). It is important to note, that as we increase the density of the material, some of the binding sites may become inaccessible; however, at this stage we do not address this issue. Analysis of the prepolymerization states of these systems as shown in Fig. 6, reveals that higher density leads to a noticeably higher proportion of

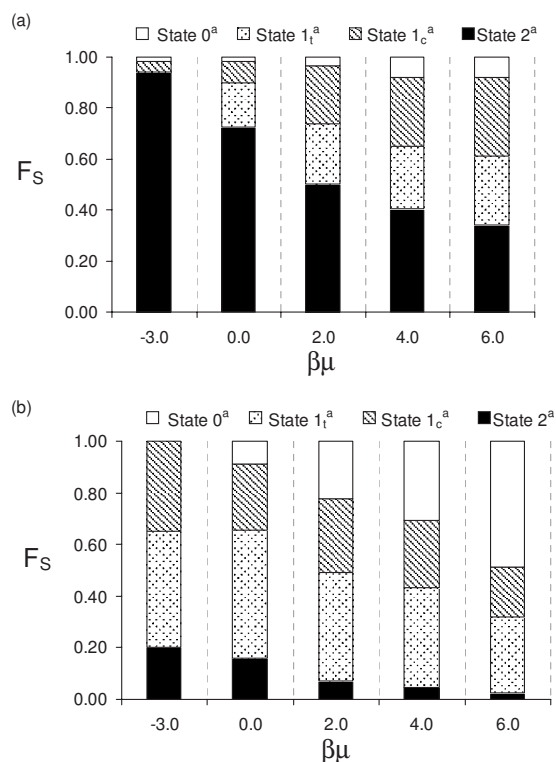


FIG. 8. Fraction F_S of adsorbed molecules in each binding state as a function of the chemical potential $\beta\mu$ in MIP3 for the template (a) and analog (b).

We perform analysis of the states of the template and analog molecules adsorbed at each point on the isotherm and observe that for MIP3 templates are predominantly adsorbed in type 2^a states for a significant part of the isotherm (Fig. 8). Although, some analogs also appear to be bound in type 2^a state, the fraction of these is relatively small throughout the isotherm. Thus, higher density leads to more specific binding sites and more pronounced molecular recognition.

Composition of the prepolymerization mixture is also a crucial optimization parameter. Both relative amounts of cross-linker and functional monomer (X:M ratio) and functional monomer and template (M:T ratio) are important and are not independent from each other. It has been observed in a number of studies that selectivity of MIPs goes through a maximum as these ratios are varied in a systematic way (for a comprehensive review of these effects, we recommend a recent article by Spivak³⁸). Here we study the effect of X:M ratio by changing the relative amounts of cross-linker and functional monomer, while maintaining the overall density of the system and the amount of the template constant. (Here $X=N_X$, $M=N_{FM1}+N_{FM2}$). We change the number of functional monomers simply by turning the cross-linker particles into functional monomers as required. The reference MIP1 has a 3:1 ratio of cross-linker to functional monomer. Three variations on this ratio are explored. MIP4 features lower number of functional monomers (X:M ratio of 7:1), MIP5 has double the number of functional monomers (X:M ratio of 1:1), and MIP6 has quadruple the number of functional monomers (X:M ratio of 0:1) compared to MIP1. Prepolymerization mixture of MIP6 consists of functional monomers and templates only, with no cross-linker particles. Therefore,

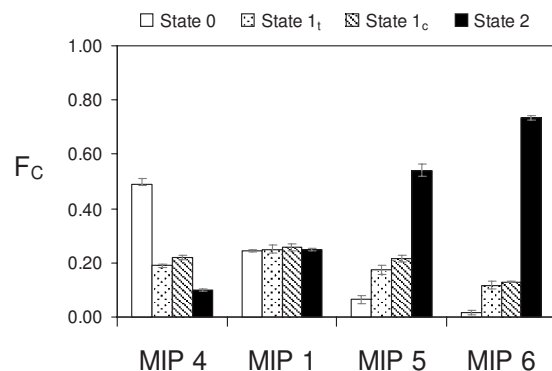


FIG. 9. Equilibrium distribution of the template-functional monomer complexes in MIP4, MIP5, and MIP6 systems prior to polymerization, compared to this distribution in MIP1.

we investigate a range of regimes from the one corresponding to the deficit of functional monomers (MIP4) to the other extreme where the whole polymer is constructed solely from the functional monomer (MIP6). As we increase the number of functional monomers in the system, the fraction of type 2 complexes also increases and this is shown in Fig. 9. In MIP6, for example, almost 75% of template molecules are in state 2 in the prepolymerization mixture. Furthermore, at a given value of the chemical potential, the selectivity of materials goes through a maximum, with MIP5, corresponding to X:M ratio of 1:1, exhibiting the highest selectivity. Figure 10 summarizes this behavior for three different values of the chemical potential. This behavior is particularly pronounced at the lower values of the chemical potential where adsorption takes place predominantly in very selective binding sites. The explanation of this maximum in selectivity is as follows. At a low concentration of the functional monomer, there are simply not enough functional monomers to form complexes of type 2 with all the available templates. As this concentration is increased, the equilibrium is shifted toward formation of type 2 complexes, leading to a larger number of highly specific 2^a binding sites. However, in the other extreme situation abundance of functional monomers leads not only to a larger number of type 2 complexes but also to a significant number of free functional monomers. Therefore,

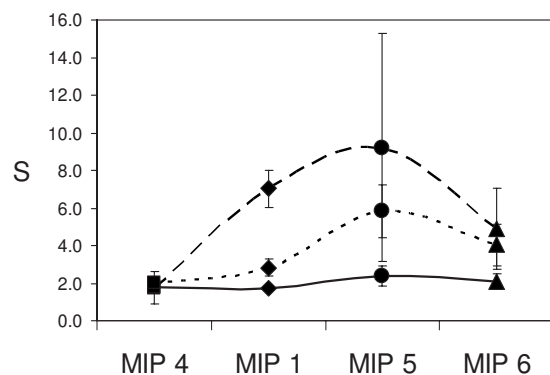


FIG. 10. Selectivity of model MIP structures as a function of cross-linker to functional monomer (X:M) ratio. From left to right: MIP4 X:M=7:1 (squares), MIP1 X:M=3:1 (diamonds), MIP5 X:M=1:1 (circles), and MIP6 X:M=0:1 (triangles). The data are plotted at three different values of the chemical potential $\beta\mu = -5.0$ (broad-dashed line), $\beta\mu = -3.0$ (dashed line), and $\beta\mu = 0.0$ (solid line).

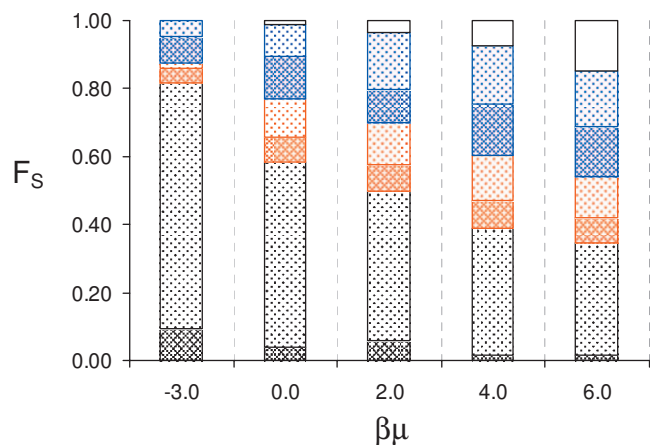


FIG. 11. (Color) Fraction F_s of adsorbed template molecules in each binding state as a function of the chemical potential $\beta\mu$ in MIP5. Color of each bar corresponds to a particular adsorbed state: gray for 2^a , blue for 1_c^a , red for 1_i^a , and white for 0^a states, respectively. Lighter shades correspond to molecules located in the binding sites, formed from the prepolymerization complexes. Darker shades correspond to molecules forming alternative associations with the matrix.

groups in real MIPs and prove to be crucial for molecular recognition to emerge in the model. Our previous models based on simpler, less specific interactions were insufficient to capture this effect.

At the heart of the model is the general simulation protocol aimed to closely mimic various stages of MIP formation and function. Equilibration of the prepolymerization mixture of components followed by quenching of the mixture and removal of the template leads to realistic imprinted structures featuring complex interconnected porous space. Thus, this approach makes it possible to explore all elements relevant to MIP performance, such as molecular recognition effects, binding sites structure, heterogeneity and distribution, pore size distribution, and connectivity within the framework of a single model. This realism of the model ensures that it is able to capture a number of experimentally observed trends. Specifically, it generates realistic values of separation factors that diminish with increased loading in accordance with experimental observations. Furthermore, the model predicts that with higher density of the material the quality of imprinting improves, leading to more specific binding sites, and hence, higher selectivity of the model MIP. We briefly explored predictions of the model for other processing conditions such as the ratio of cross-linker to functional monomer in the prepolymerization mixture. The model predicts a maximum in the selectivity of model materials, as this ratio is varied. At low concentration of the functional monomers, there is simply not enough monomers to form complexes with all available templates. On the other hand, very high concentrations of the functional monomer result in predominantly nonspecific binding. This is in agreement with experimental observations, although an additional factor noticed in experiments is lower rigidity and robustness of the polymer network at high concentrations of the functional monomer.³⁹ In general, this is an encouraging result as the model demonstrates the capability to assess the role of various processing conditions in the final properties of MIPs, and therefore it can be used to provide some qualitative insights on the optimal values of processing parameters.

We expect that the model can make a particular important contribution to our understanding of molecular recognition mechanisms in MIPs. In the range of conditions explored in this work, we consistently observe that the analog molecules are able to form very favorable associations with the matrix even though the porous space is imprinted to recognize the interaction pattern of the template. This is an important contribution to a diminished selectivity of MIPs, highlighted by this model.

Several aspects of the model require further development. In the current version the polymerization process is modeled simply by quenching molecules of the prepolymerization mixture in their instant locations and orientations. A more realistic approach would involve some mechanism of association between cross-linkers and functional monomers. This model would be able to generate connected and self-sustaining polymer networks. This can be easily implemented using the same language of surface interaction sites that we use to describe functional monomer–functional group associations. Furthermore, in this study we do not ad-

additional opportunities open for the analog to form two associations (state 2^a) upon adsorption. This limits the effect of the imprinting on the structure and the resulting MIP exhibits less specific binding.

It is also interesting to examine the nature of binding states of adsorbed molecules in the imprinted materials. Specifically, we would like to assess how many molecules in a particular state are actually located in the binding sites evolved from the corresponding complexes in the prepolymerization mixture. For this, in Fig. 11, we consider the most selective material MIP5 and, in addition to the original distribution of adsorbed molecules among various binding states, we also delineate between *rebinding* to the original binding sites (lighter patterns) and forming new associations, not observed during the prepolymerization (darker patterns). For example, at the chemical potential $\beta\mu = -3.0$ about 81% of all adsorbed molecules are in 2^a state (gray patterns), but about 9% are in 2^a binding sites that did not form from type 2 complexes during the imprinting process. About 5% of molecules are in state 1_i^a (red patterns), but only 1% are in the binding sites formed from 1_i complexes, and about 14% of adsorbed molecules are in 1_c^a state (blue patterns), but only 4% are located in the binding sites formed from 1_c complexes. This analysis indicates that about 10% of the most specific binding sites identified from a typical binding site distribution method, such as the Freundlich isotherms, may not have originated from imprinting.

IV. CONCLUSIONS

In this article we propose a simple model of imprinted porous materials. For the first time, molecular recognition effect emerges in the model of MIPs. Molecular species in this model are treated as either hard spheres or rigid clusters of hard spheres. Some of the hard spheres also feature small interaction sites capable of associating with each other in a prescribed manner. These associations aim to imitate interactions between the functional monomers and functional

dress the accessibility of the binding sites, and this is an important factor to be investigated in our future work. It is also important to explore molecular recognition effects as a function of molecular geometry. Our preliminary studies on the systems with a single type of functional monomer and a single functional group (the analog then differs from the template by the location of the functional group) suggest that the main conclusions of this work remain valid for this simpler case; however, the magnitude of the observed separation factors is lower. Therefore, the main focus of the future work will be on more complex systems, where one might expect a richer spectrum of behavior.

ACKNOWLEDGMENTS

The authors thank the Engineering and Physical Sciences Research Council for financial support through Grant No. EP/D074762/1. This work has made use of the resources provided by the Edinburgh Compute and Data Facility (ECDF). (<http://www.ecdf.ed.ac.uk/>). The ECDF is partially supported by the eDIKT initiative (<http://www.edikt.org.uk>). The authors thank Professor Simcha Srebnik for useful discussions and advise.

- AQ: #1** ¹ Polyakov, Zh. Fiz. Khim. **■**, 799 (1931).
² C. Alexander, H. S. Andersson, L. I. Andersson, R. J. Ansell, N. Kirsch, I. A. Nicholls, J. O'Mahony, and M. J. Whitcombe, *J. Mol. Recognit.* **19**, 106 (2006).
³ G. Vlatakis, L. I. Andersson, R. Müller, and K. Mosbach, *Nature (London)* **361**, 645 (1993).
⁴ P. A. G. Cormack and A. Z. Elorza, *J. Chromatogr. B Analyt. Technol. Biomed. Life Sci.* **804**, 173 (2004).
⁵ R. J. Umpleby, S. C. Baxter, A. M. Rampey, G. T. Rushton, Y. Chen, and K. D. Shimizu, *J. Chromatogr. B Analyt. Technol. Biomed. Life Sci.* **804**, 141 (2004).
⁶ I. A. Nicholls, *Chem. Lett.* **■**, 1035 (1995).
⁷ I. A. Nicholls, K. Adbo, H. S. Andersson, P. O. Andersson, J. Ankarloo, J. Hedin-Dahlstrom, P. Jokela, J. G. Karlsson, L. Olofsson, J. Rosengren, S. Shoravi, J. Svenson, and S. Wikman, *Anal. Chim. Acta* **435**, 9 (2001).

- ⁸ B. Sellergren, M. Lepisto, and K. Mosbach, *J. Am. Chem. Soc.* **110**, 5853 (1988).
⁹ H. S. Andersson, A. C. KochSchmidt, S. Ohlson, and K. Mosbach, *J. Mol. Recognit.* **9**, 675 (1996).
¹⁰ M. J. Whitcombe, L. Martin, and E. N. Vulfson, *Chromatographia* **47**, 457 (1998).
¹¹ I. Chianella, M. Lotierzo, S. A. Piletsky, I. E. Tothill, B. N. Chen, K. Karim, and A. P. F. Turner, *Anal. Chem.* **74**, 1288 (2002).
¹² K. Karim, F. Breton, R. Rouillon, E. V. Piletska, A. Guerreiro, I. Chianella, and S. A. Piletsky, *Adv. Drug Delivery Rev.* **57**, 1795 (2005).
¹³ S. Srebnik and O. Lev, *J. Chem. Phys.* **116**, 10967 (2002).
¹⁴ S. Srebnik, *Chem. Mater.* **16**, 883 (2004).
¹⁵ I. Yungerman and S. Srebnik, *Chem. Mater.* **18**, 657 (2006).
¹⁶ X. Y. Wu, W. R. Carroll, and K. D. Shimizu, *Chem. Mater.* **20**, 4335 (2008).
¹⁷ S. A. Piletsky, K. Karim, E. V. Piletska, C. J. Day, K. W. Freebairn, C. Legge, and A. P. F. Turner, *Analyst (Cambridge, U.K.)* **126**, 1826 (2001).
¹⁸ I. Chianella, M. Lotierzo, S. A. Piletsky, I. E. Tothill, B. Chen, K. Karim, and A. P. F. Turner, *Anal. Chem.* **74**, 1288 (2002).
¹⁹ I. Chianella, K. Karim, E. V. Piletska, C. Preston, and S. A. Piletsky, *Anal. Chim. Acta* **559**, 73 (2006).
²⁰ D. Pavel and J. Lagowski, *Polymer* **46**, 7543 (2005).
²¹ D. Pavel, J. Lagowski, and C. J. Lepage, *Polymer* **47**, 8389 (2006).
²² D. Pavel and J. Lagowski, *Polymer* **46**, 7528 (2005).
²³ S. Monti, C. Cappelli, S. Bronco, P. Giusti, and G. Ciardelli, *Biosens. Bioelectron.* **22**, 153 (2006).
²⁴ G. Ciardelli, C. Borrelli, D. Silvestri, C. Cristallini, N. Barbani, and P. Giusti, *Biosens. Bioelectron.* **21**, 2329 (2006).
²⁵ D. B. Henthorn and N. A. Peppas, *Ind. Eng. Chem. Res.* **46**, 6084 (2007).
²⁶ L. Sarkisov and C. Herdes, *Langmuir* (unpublished).
²⁷ P. R. Van Tassel, *Phys. Rev. E* **60**, R25 (1999).
²⁸ L. H. Zhang and P. R. Van Tassel, *Mol. Phys.* **98**, 1521 (2000).
²⁹ L. H. Zhang and P. R. Van Tassel, *J. Chem. Phys.* **112**, 3006 (2000).
³⁰ L. H. Zhang, S. Y. Cheng, and P. R. Van Tassel, *Phys. Rev. E* **64**, 044101 (2001).
³¹ S. Cheng and P. R. Van Tassel, *J. Chem. Phys.* **114**, 4974 (2001).
³² L. Sarkisov and P. R. Van Tassel, *J. Phys. Chem. C* **111**, 15726 (2007).
³³ L. Sarkisov and P. R. Van Tassel, *J. Chem. Phys.* **123**, (2005).
³⁴ R. Spori and L. Sarkisov, *Characterization of Porous Solids VIII* (■, ■, 2009), p. 204.
³⁵ J. Kolafa and I. Nezbeda, *Mol. Phys.* **61**, 161 (1987).
³⁶ I. Nezbeda, J. Kolafa, and Y. V. Kalyuzhnyi, *Mol. Phys.* **68**, 143 (1989).
³⁷ R. Q. Snurr, A. T. Bell, and D. N. Theodorou, *J. Phys. Chem.* **97**, 13742 (1993).
³⁸ D. A. Spivak, *Adv. Drug Delivery Rev.* **57**, 1779 (2005).
³⁹ B. Sellergren, *Macromol. Chem. Phys.* **190**, 2703 (1989).

AUTHOR QUERIES — 056921JCP

- #1 Au: Please supply authors initial and volume in Ref. 1.
- #2 Au: Please supply volume number in Ref. 6.
- #3 Au: Please update Ref. 26.
- #4 CrossRef reports the author should be "Zhang, Paul R. Van Tassel" not "Zhang" in the reference 28 "Zhang, Van Tassel, 2000".
- #5 Au: Please update volume, page, year for Ref. 30
- #6 Au: Please supply publisher and location in Ref. 34.